ORGANIC CHEMISTRY

Cu(II) carboxylate arene C—H functionalization: Tuning for nonradical pathways

Fanji Kong[1], Shusen Chen[2], Junqi Chen[1], Chang Liu[1], Weihao Zhu[1], Diane A. Dickie[1], William L. Schinski[3], Sen Zhang[1], Daniel H. Ess[2]*, T. Brent Gunnoe[1]*

We report carbon-hydrogen acetoxylation of nondirected arenes benzene and toluene, as well as related functionalization with pivalate and 2-ethylhexanoate ester groups, using simple copper(II) [Cu(II)] salts with over 80% yield. By changing the ratio of benzene and Cu(II) salts, 2.4% conversion of benzene can be reached. Combined experimental and computational studies results indicate that the arene carbon-hydrogen functionalization likely occurs by a nonradical Cu(II)-mediated organometallic pathway. The Cu(II) salts used in the reaction can be isolated, recycled, and reused with little change in reactivity. In addition, the Cu(II) salts can be regenerated in situ using oxygen and, after the removal of the generated water, the arene carbon-hydrogen acetoxylation and related esterification reactions can be continued, which leads to a process that enables recycling of Cu(II).

INTRODUCTION

As an important industrial chemical, phenol has been deployed in applications in various fields including household products, nylon, polymers, and the manufacturing of other chemical derivatives. Over 12 million metric tons of phenol are produced each year, and greater than 90% of phenol is produced through the Hock process (*1*–*2*). However, a major issue with the Hock process is the generation of a stoichiometric amount of acetone as an oversupplied side product (*1*). Alternative methods for phenol production include a three-step route from benzene to phenol with cyclohexanone as a coproduct developed by ExxonMobil and the oxidation of benzene using N_2O developed by Solutia (*3*–*5*). However, the source of N_2O gas limits the location and amount of phenol production for the Solutia process, while neither of the other methods provide a desirable coproduct-free route for phenol production (Fig. 1). Other related benzene hydroxylation processes using copper rely on the formation of hydroxyl radical and/or require solid supports to form heterogeneous catalysts (*2*, *6*–*8*), which suffer from low selectivity and/or low yield.

Acetoxylation of benzene has been considered as a potential route for phenol production since hydrolysis of phenyl acetate generates phenol (*9*). Palladium-catalyzed benzene acetoxylation has been studied (*10*–*11*), but only a limited number of examples of aromatic C—H acetoxylation/hydroxylation have been reported using low-cost transition metals, and these examples rely on functionalized aromatic substrates with "directing groups" to facilitate coordination to the catalyst (*12*–*19*). Yu and co-workers (*12*) demonstrated a series of C—H functionalizations using pyridine as the directing group with copper(II) acetate as the catalyst precursor, and the reaction was proposed to occur by the formation of a radical cation intermediate via a single electron transfer mechanism. Later, the Shi group (*13*) reported a study using a bidentate directing group derived from 2-(pyridine-2-yl)isopropylamine through a proposed Cu(III)-aryl intermediate. Subsequently, the Yu group (*15*) demonstrated a related C—H hydroxylation process using oxazolyamide as the directing group via a possible monomeric Cu(III)-aryl intermediate. Benzoic acid has also been reported as a directing group for the synthesis of hydroxylated arenes assisted by benzoyl peroxide (*17*). Other related C—H functionalization processes by Cu(II) also require a directing group to facilitate the reaction (*20*–*31*).

To our knowledge, there are no reported examples of molecular Cu(II)-mediated arene acetoxylation without directing groups on the arene. Here, we report acetoxylation of benzene and toluene using simple Cu(II) salts, and we propose that the C—H functionalization occurs by a nonradical organometallic pathway that forms Cu-aryl intermediates under certain conditions. The Cu(II) salt offers recyclability using O_2 or air, similar to the commercialized Pd-catalyzed ethylene oxidation Wacker process that has proven viable with Cu(II) recycling both in situ (with purified O_2) and in a separate step/reactor from the ethylene oxidation process (using air) (*32*–*35*). This process can potentially lead to a coproduct-free synthetic route for phenol production (Fig. 1), since all of the coproducts are used for recycling of the Cu(II) salt, and, thus, the overall reaction is the conversion of benzene and dioxygen to phenol (Fig. 1).

RESULTS

Development of nondirected Cu(II)-mediated C—H acetoxylation of benzene

Phenyl acetate has been observed as a side product in our previously reported Rh-catalyzed arene alkenylation that incorporates $Cu(OAc)_2$. Phenyl acetate formation is the result of a reaction of $Cu(OAc)_2$ with benzene (*36*). After initial optimization of conditions (sections S2 and S3), we found that heating (180°C) 10 ml of a benzene mixture with predried $Cu(OAc)_2$ [0.48 mole percent (mol %) relative to benzene] under dinitrogen [75 psig (pound-force per square inch gauge)] produces phenyl acetate in 87(1)% yield based on the Cu(II)-limiting reagent as determined by gas chromatography with flame ionization detection (GC-FID) (Table 1, entry 2). The control experiment using $CuCl_2$ showed no activity for C—H activation on benzene (Table 1, entry 12), which likely indicates that the carboxylate group is essential for arene C—H activation (see below). Similar to $Cu(OAc)_2$, more soluble Cu(II) salts, such as Cu(II) pivalate [$Cu(OPiv)_2$] and Cu(II) 2-ethylhexanoate [$Cu(OHex)_2$], were shown to achieve similar reactions at even a lower temperature (Table 1, entries 6, 7, and

[1]Department of Chemistry, University of Virginia, Charlottesville, VA 22904, USA. [2]Department of Chemistry and Biochemistry, Brigham Young University, Provo, UT 84604, USA. [3]2818 Las Gallinas Ave. San Rafael, CA 94903.
*Corresponding author. Email: tbg7h@virginia.edu (T.B.G.); dhe@chem.byu.edu (D.H.E.)

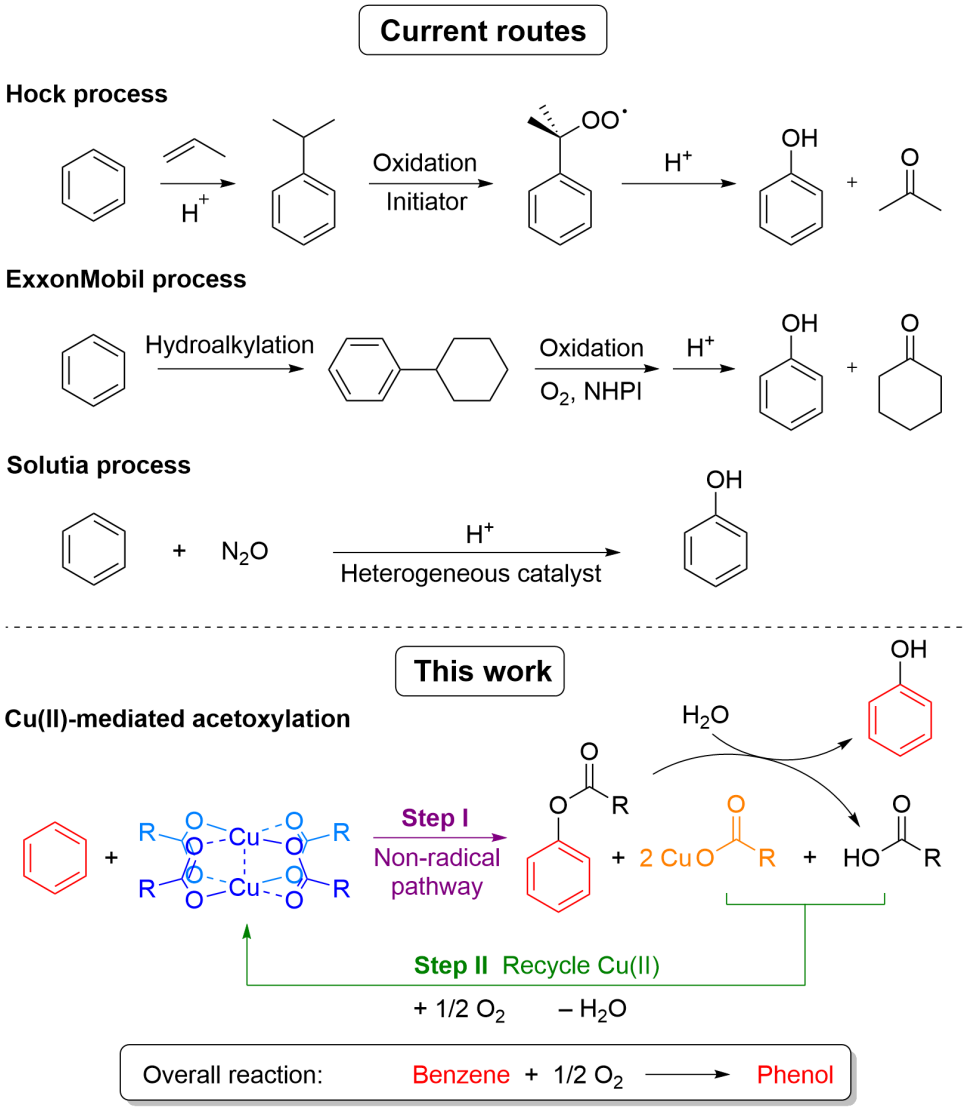

Fig. 1. Current methods for phenol production and the proposed method via Cu(II)-mediated acetoxylation. NHPI, *N*-hydroxyphthalimide.

9). The Cu(II) species $Cu(OPiv)_2$ was found to give a lower yield compared to the other Cu(II) salts, which we attribute to the lower thermostability of the pivalic group (section S2.5). The presence of air was found to inhibit the reaction (Table 1, entry 4), and the reaction was slowed down with the addition of an increasing amount of carboxylic acid (Table 1, entries 3, 5, 8, 10, and 11). Different ligands and solvents were tested for the reaction; however, none of them provided a beneficial effect (sections S5.1 and S6). These observations are distinct from the previously published directed Cu(II)-mediated acetoxylation processes (*12*, *14*–*19*), in which the presence of acid, air, or ligands is commonly required by the reactions.

Mechanistic studies

To differentiate between radical and nonradical pathways, separate reactions of toluene or a mixture of benzene with cyclohexane were used as probes. These reactions offer intramolecular and intermolecular competition of weaker sp^3 C—H bonds and stronger sp^2 C—H bonds (Fig. 2, A and B). It is expected that a radical C—H abstraction reaction will select for the weaker sp^3 C—H bonds. Under anhydrous conditions, all of the reactions were found to select for the stronger sp^2 C—H bonds, which suggests that the reactions likely undergo a nonradical reaction pathway. Using 1 ml of benzene with 9 ml of cyclohexane resulted in ~10% of the rate compared to the reaction using neat benzene, consistent with the reaction being first order in benzene. A common radical trap, (2,2,6,6-tetramethylpiperidin-1-yl)oxyl (TEMPO), was tested as an additive in the reaction of toluene with $Cu(OAc)_2$ (Fig. 2C). The reactions with TEMPO were slow and remained selective for tolyl acetates, but more benzyl acetate was formed compared to reactions without TEMPO. In a control experiment, we found that TEMPO can functionalize the benzylic position of toluene without Cu(II) salt (Fig. 2D). When using toluene as the substrate, the regioselectivity of the sp^2 C—H bonds can be used to differentiate between a potential electrophilic aromatic substitution mechanism ($^{Ar}S_E$, with no M—C bond formation) and a metal-mediated C—H activation mechanism via M—C bond formation (*37*–*38*). The Cu(II)-mediated reaction was found to be more selective

Table 1. Selected results for benzene acetoxylation and related reactions using Cu(II) salts. Yield of the phenyl carboxylate is relative to the limiting reagent (CuX_2) as determined by GC-FID. The theoretical maximum conversion of benzene will be 0.24%. Reaction conditions: benzene (10 ml, 112.3 mmol), CuX_2 (0.48 mol %, 0.540 mmol), 75 psig of N_2. CuX_2 = $Cu(OAc)_2$ anhydrous; $Cu(OPiv)_2$ or $Cu(OHex)_2$. N.D., not detected. SDs were calculated from at least three independent experiments.

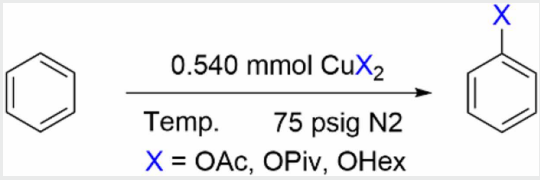

Entry	Cu(II) salt	Temp. (°C)	HX (equiv.)	Air	Yield (%)	Time (hours)
1	$Cu(OAc)_2$	180	0	None	78(0)	24
2	$Cu(OAc)_2$	180	0	None	87(1)	40
3	$Cu(OAc)_2$	180	1.0	None	80(1)	40
4*	$Cu(OAc)_2$	180	0	1 atm	15(2)	24
5	$Cu(OAc)_2$	180	4.0	None	65(6)	48
6	$Cu(OPiv)_2$	180	0	None	49(1)	16
7	$Cu(OPiv)_2$	170	0	None	52(0)	16
8	$Cu(OPiv)_2$	170	1.0	None	36(1)	16
9	$Cu(OHex)_2$	170	0	None	89(1)	24
10	$Cu(OHex)_2$	170	1.0	None	71(1)	40
11	$Cu(OHex)_2$	170	4.0	None	37(0)	72
12†	$CuCl_2$	180	0	None	N.D.	24

*Using 1 atm of air, the total top pressure of air and N_2 is 75 psig. †Using half the amount of reagents in a custom made high-pressure steel reactor with Swagelok Vacuum Coupling O-ring (VCO) seal fitting reactor under 100 psig of Ar.

for the meta-tolyl carboxylate than the ortho-tolyl carboxylate (Table 2, entries 1, 4, and 5), which we propose (see below) is a result of an organometallic reaction that forms Cu-tolyl intermediates. We propose that the Cu-mediated toluene C—H activation favors the meta-position over the ortho-position of toluene due to the steric effect of the methyl group.

In the presence of 1 atm of dried O_2, the selectivity of toluene acetoxylation reaction using $Cu(OAc)_2$ changed to form benzyl acetate (Table 2, entry 3), which is evidence for a radical process since the weaker benzyl C—H bond was functionalized. In addition, the inclusion of O_2 suppresses reactivity with the stronger sp^2 tolyl C—H bonds, similar to our observation when using benzene as the substrate that exhibited lower yield in the presence of O_2 (Table 1, entry 4). The selectivity shifts from sp^2 C—H bond functionalization to benzylic functionalization is expected since mixing Cu(II) with O_2 is known to form Cu-peroxo and/or superoxo species (*39*–*42*), which likely leads to the formation of free radical species that favor weaker sp^3 C—H bond functionalization over stronger sp^2 C—H bonds. Since hexamethylbenzene (HMB), which has been used as the standard for GC analysis, contains benzylic C—H bonds and the Cu(II)-mediated functionalization of toluene activates benzyl C—H bonds under some conditions, control experiments were done using $Cu(OAc)_2$ and toluene as the substrate at 180°C with in situ and ex situ addition of HMB for GC-FID analysis (fig. S6). As expected, under anaerobic conditions, the consumption of HMB is negligible, while under aerobic conditions, a competing radical-based reaction with HMB was observed, which is consistent with our proposal that reaction pathways are distinct under anaerobic versus aerobic conditions. Therefore, to avoid complications caused by the consumption of HMB, all the reported quantifications used ex situ addition of HMB for GC analysis. Water was also examined as an additive (Table 2, entries 4 and 11), and similar to O_2, the presence of 1 equivalent of water (relative to Cu) switches the reaction selectivity for toluene activation toward benzylic C—H functionalization, although tolyl products are still observed (section S11). We suspect that water coordinates to $Cu_2(\mu\text{-}OAc)_4$ to form copper(II) acetate hydrate, $Cu_2(\mu\text{-}OAc)_4{\cdot}2H_2O$, which can convert to monomeric $Cu(OAc)_2{\cdot}(H_2O)_n$ (*43*) or other decomposition species such as Cu/Cu_2O under reaction temperatures that could lead to a radical process(es) that competes with the organometallic Cu(II)-mediated pathway. The observation of a similar change in reaction selectivity using commercial copper(II) acetate monohydrate [$Cu_2(\mu\text{-}OAc)_4{\cdot}2H_2O$] (Table 2, entry 5) is consistent with the observation of reactions with water added to anhydrous $Cu_2(\mu\text{-}OAc)_4$. The addition of increasing amounts of carboxylic acid (Table 2, entries 6 and 12 to 14) decreases the reaction rate without changing the benzyl-to-tolyl selectivity. This suggests that carboxylic acid inhibits the organometallic reaction pathway but does not facilitate undesirable radical-based processes, which is different from the effect of water or O_2.

The presence of bi- or tridentate ligand [e.g., bipyridine, terpyridine, tetramethyl ethylenediamine, and 1,2-bis(dimethylphosphino)ethane] shuts down the benzene functionalization reaction, and many ligands result in a switch of the reaction selectivity for toluene activation toward benzylic C—H functionalization (section S5.1). However, using

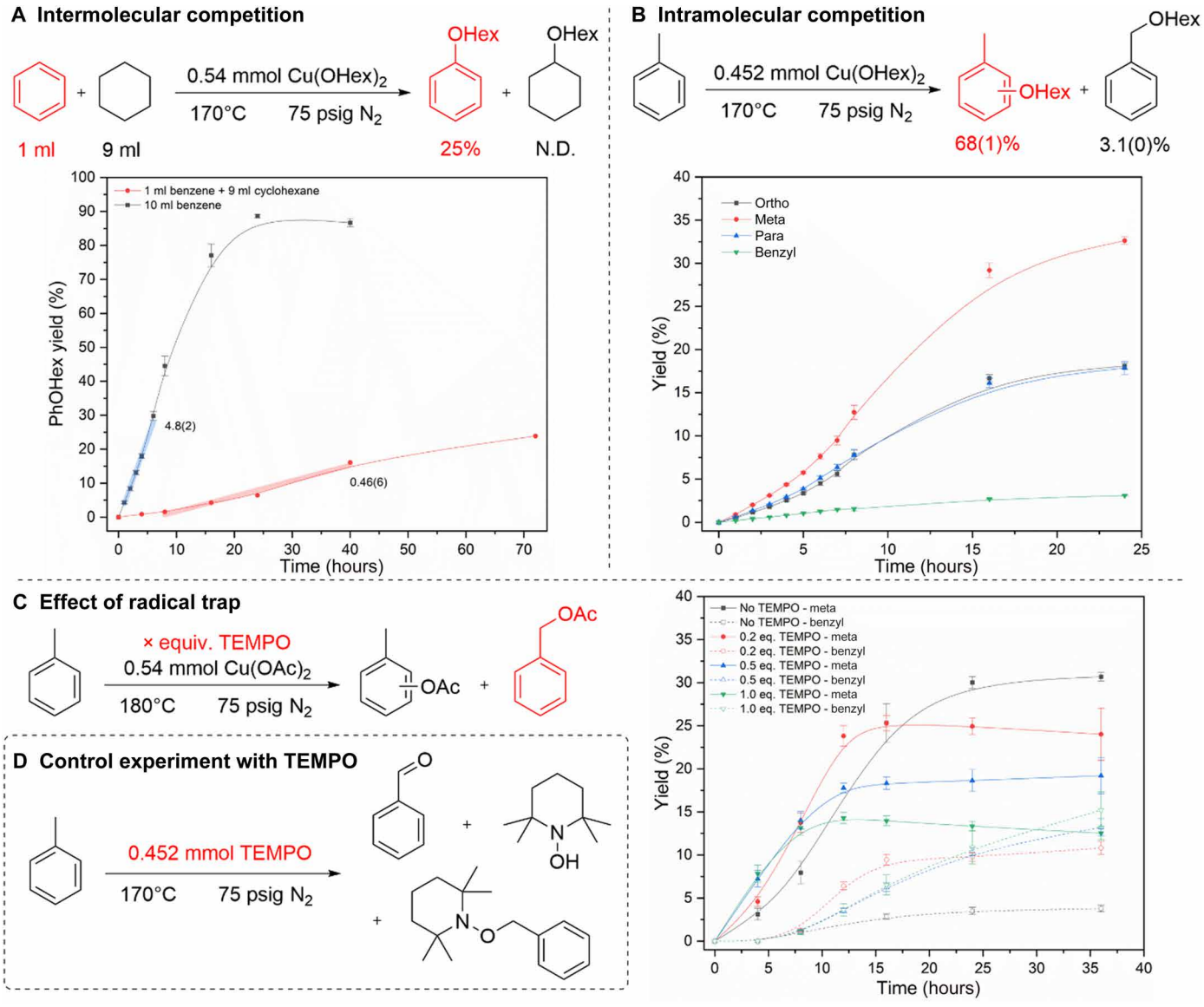

Fig. 2. Differentiate between radical and nonradical pathways. (**A**) Intermolecular competition of sp^2 versus sp^3 C—H bonds using a mixture of benzene and cyclohexane. N.D., not detected. (**B**) Intermolecular competition of sp^2 versus sp^3 C—H bonds using toluene. (**C**) Meta-tolyl acetate and benzyl acetate yield versus time plot of reaction using different amounts of TEMPO. Reaction conditions: toluene (10 ml, 94.1 mmol), $Cu(OAc)_2$ (98 mg, 0.540 mmol), TEMPO [0, 0.2, 0.5, and 1.0 equiv. relative to $Cu(OAc)_2$], under 75 psig of N_2 at 180°C. (**D**) Observed products of control experiment using TEMPO with no Cu(II) salt. Reaction conditions: toluene (10 ml, 94.1 mmol), TEMPO (71 mg, 0.452 mmol), under 75 psig of N_2 at 170°C. SDs were calculated from at least three independent experiments.

$(MeO)_3P{=}O$, which we presume is a weakly coordinating ligand, only slows down the arene functionalization process without changing the sp^2-to-sp^3 selectivity (Fig. 3A). By refluxing $Cu(OAc)_2$ and $(MeO)_3P{=}O$ in toluene, the resulting product was found to be the bis-Cu complex $[(MeO)_3P{=}O]_2Cu_2(\mu\text{-}OAc)_4$. The structure of $[(MeO)_3P{=}O]_2Cu_2(\mu\text{-}OAc)_4$ was confirmed by a single-crystal x-ray diffraction study (Fig. 3B). We speculate that $(MeO)_3P{=}O$ does not disrupt the dimeric Cu(II) structure and hence only slows down the functionalization of arenes by competing with the arene substrate for Cu coordination. In contrast, multidentate ligands likely convert bis-Cu(II) to monomeric Cu(II) complexes of the type $LCu^{II}X_2$ that are not active for the functionalization of arenes (Fig. 4A). By monitoring the initial rate of the reaction using different amounts of soluble $Cu_2(\mu\text{-}OHex)_4$ and 2-ethylhexanoic acid (HOHex), the reaction was found to be first order in $Cu_2(\mu\text{-}OHex)_4$ concentration (fig. S26) and inverse first order in HOHex concentration (fig. S29). On the basis of these observations, we propose a plausible reaction pathway and rate equation (Fig. 4B). Reversible arene C—H activation by $Cu_2(\mu\text{-}X)_4$ (X = OAc, OHex, or OPiv) and dissociation of carboxylic acid are followed by an overall rate-limiting reductive coupling/elimination of aryl ester. This proposed reaction pathway is consistent with the results of density functional theory (DFT) calculations (see below).

On the basis of the proposed rate equation (Fig. 4B), the rate constant for the C—H activation step (k_1) can be calculated via a curve fitting of rate versus [HOHex] (Fig. 5C) or the intercept from a 1/rate versus [HOHex] plot (fig. S31), where rate is the slope of the

Table 2. Selected results for toluene acetoxylation and related reactions using simple Cu(II) salts. Yield of the tolyl or benzyl carboxylate is relative to the limiting reagent (CuX_2). Reaction conditions: toluene (10 ml, 94.1 mmol), CuX_2 [for $Cu(OAc)_2$, 0.57 mol %, 0.540 mmol; for $Cu(OPiv)_2$ or $Cu(OHex)_2$, 0.48 mol %, 0.452 mmol), under 75 psig of N_2. $CuX_2 = Cu(OAc)_2$ anhydrous, $Cu(OPiv)_2$, or $Cu(OHex)_2$. SDs were calculated from at least three independent experiments.

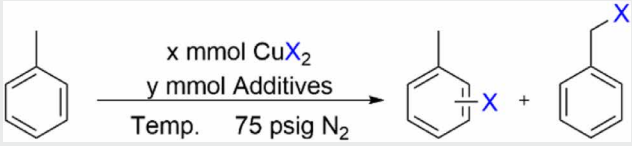

Entry	CuX_2	Temp. (°C)	Additive (equiv.)	Yield (%)					Time (hours)
				Total	Benzyl	Para	Meta	Ortho	
1	$Cu(OAc)_2$	180	None	72(1)	4.0(5)	19(0)	31(1)	18(0)	40
2	$Cu(OAc)_2$	170	None	71(2)	5.0(2)	20(1)	31(1)	15(1)	96
3*	$Cu(OAc)_2$	180	Dried O_2	95(6)	89(6)	1(0)	3(0)	2(0)	4
4	$Cu(OAc)_2$	180	H_2O (1.0)	37(2)	17(2)	5(0)	10(0)	5(0)	40
5	$Cu(OAc)_2{\cdot}H_2O$	180	None	48(3)	23(0)	7(1)	13(2)	6(1)	96
6	$Cu(OAc)_2$	180	HOAc (1.0)	50(3)	3.0(3)	12(1)	23(2)	11(1)	40
7	$Cu(OAc)_2$	180	Ac_2O (1.0)	3(1)	0.3(0)	1(0)	2(0)	1(0)	24
8	$Cu(OPiv)_2$	170	None	33(0)	0.9(1)	10(0)	16(0)	7(0)	16
9	$Cu(OHex)_2$	180	None	54(1)	2.4(2)	16(0)	24(0)	12(0)	8
10	$Cu(OHex)_2$	170	None	72(0)	3.1(1)	18(1)	33(1)	18(0)	24
11	$Cu(OHex)_2$	170	H_2O (1.0)	41(3)	8.4(0)	9(1)	16(2)	7(1)	24
12	$Cu(OHex)_2$	170	HOHex (1.0)	68(2)	2.9(1)	19(1)	33(1)	13(0)	40
13	$Cu(OHex)_2$	170	HOHex (2.0)	56(1)	2.8(3)	15(0)	28(1)	10(3)	40
14	$Cu(OHex)_2$	170	HOHex (4.0)	36(1)	2.3(2)	10(0)	19(1)	6(1)	48

*Using 1 atm of dried O_2, the total top pressure of O_2 and N_2 is 75 psig.

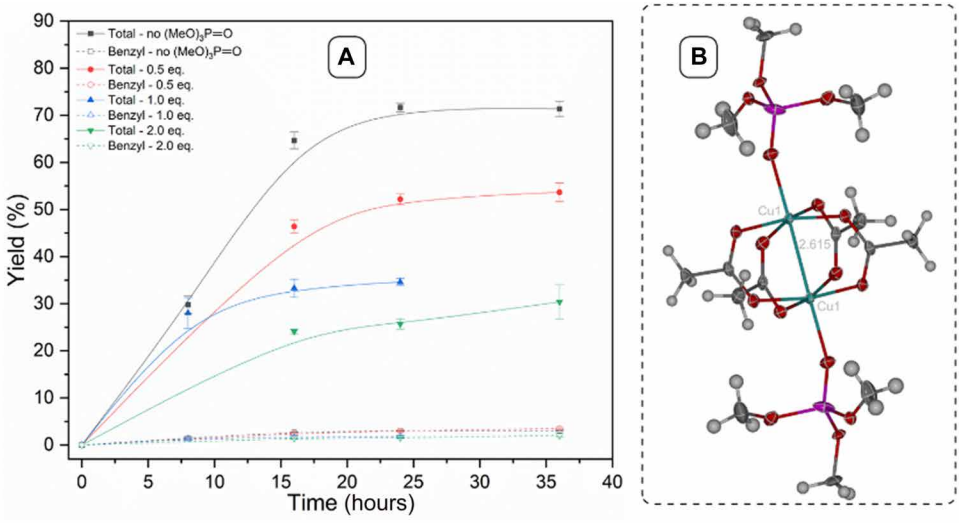

Fig. 3. Effects of weakly coordinating $(MeO)_3P{=}O$ ligands. (**A**) Sum of tolyl/benzyl OHex yields and benzyl OHex yield versus time plot with the presence of different amounts of $(MeO)_3P{=}O$ ligands. Reaction conditions: toluene (10 ml, 94.1 mmol), $Cu(OHex)_2$ (0.48 mol %, 0.452 mmol), $(MeO)_3P{=}O$ (0, 0.5, 1.0, and 2.0 equiv. relative to $Cu(OHex)_2$), under 75 psig of N_2 at 170°C. SDs were calculated from at least three independent experiments. (**B**) Oak Ridge thermal ellipsoid plot of $\{(MeO)_3P{=}O\}_2Cu_2(\mu\text{-}OAc)_4$. Ellipsoids are drawn at 50% probability level.

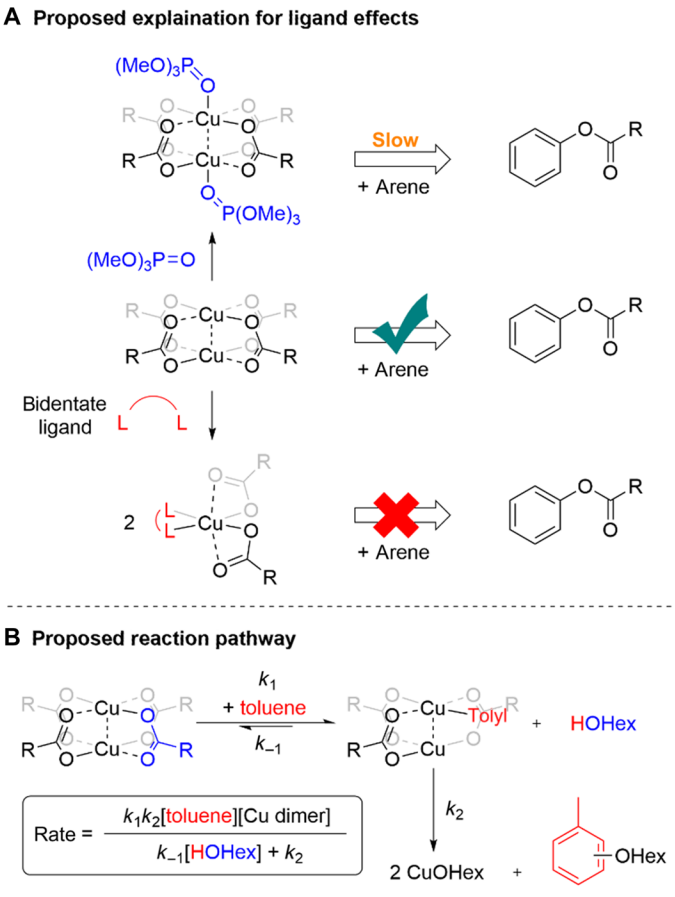

Fig. 4. Ligand effects and reaction pathway. (**A**) Proposed competing pathway in the arene acetoxylation reaction in the presence of weakly coordinating or bidentate ligand. (**B**) Proposed reaction pathway and associated rate law.

concentration of tolyl OHex versus time plot (fig. S28). Both plots gave good fits, which is consistent with the proposed reaction pathway. The rate constant for the C—H activation step (k_1) and the related activation free energy ($\Delta G_1^{\ddagger}{}_{443K}$) can be estimated from the intercept as 2.7(4) 10^{-6} s^{-1} M^{-1} and 38(1) kcal mol^{-1} (section S9). A slight induction period was observed for all of the Cu(II)-mediated acetoxylation reactions without addition of carboxylic acid. The reaction rates of the induction period and the initial linear region were monitored at different reaction temperatures using soluble $Cu(OHex)_2$ with toluene as the substrate (fig. S23 and table S11). It was found that a decrease in reaction temperature led to an increase in the induction period, and at 180°C, there is no observable induction period. The induction period of the reaction was also studied in the presence of variable concentrations of HOHex (fig. S24), and with the addition of more acid, the induction period becomes less obvious. We propose that the induction period is due to the process of dissolving Cu(II) salt under acid-free conditions.

To gain insight into the Cu(II)-mediated arene C—H activation step, we studied the kinetic isotope effect (KIE) using C_6H_6 and C_6D_6 as the substrates with soluble $Cu(OHex)_2$ at 170°C. The KIE value was determined to be 3.0(1) for parallel reactions using benzene and benzene-d_6 and 2.8(1) for the intermolecular competition reactions using a mixture of benzene and benzene-d_6 with a 1-to-1 molar ratio (Fig. 5A). This type of KIE has typically been interpreted as C—H cleavage that occurs during or before the rate-determining step (*44*–*45*), which is consistent with the proposed reaction pathway (Fig. 4B). In the presence of eight equivalents of DOAc [relevant to $Cu(OAc)_2$], a small amount of deuterium incorporation (3.0(3)%) was found in the product (Fig. 5B), which likely indicates that the C—H activation step is partially reversible and is also consistent with the proposed reaction pathway (Fig. 4B).

An Eyring analysis was performed using reaction rates measured at seven temperatures between 150° and 180°C (Fig. 5D, in black), which provided an activation enthalpy ($\Delta H^{\ddagger}$) of 38(1) kcal mol^{-1}. The activation entropy ($\Delta S^{\ddagger}$) was found to be −1(3) cal mol^{-1} K^{-1} assuming an overall second-order rate law (rate = k''_{obs}[toluene][Cu_2(μ-OHex)$_4$]), which indicates that the entropy has a negligible effect on the overall reaction. The small entropy of activation is potentially due to the use of excess toluene as the solvent and/or that the C—H activation step may only be partially rate limiting (see DFT calculations below). Using an Arrhenius plot (fig. S47), the activation energy (E_a) was determined to be 39(1) kcal mol^{-1}. As described above, the rate constant of the C—H activation step (k_1) can be determined; therefore, a set of reactions has been done over the temperature range of 150° to 180°C under the conditions with addition of variant amounts of HOHex to calculate k_1 at different temperatures (table S25). The Eyring analysis performed using k_1 at different temperatures as it shown in Fig. 5D (in red), and these data indicate a $\Delta H^{\ddagger}$ of 29(2) kcal mol^{-1} and a $\Delta S^{\ddagger}$ of −19(4) cal mol^{-1} K^{-1}. These activation parameters are consistent with the proposed mechanism for arene C—H activation and the results of computational modeling (see below).

Computational modeling

To further understand the reaction mechanism, we used DFT and time-dependent (TD)–DFT calculations to examine closed-shell (C—H activation) and open-shell (e.g., electron transfer, hydrogen atom transfer, and proton-coupled electron transfer; section S16) reaction pathways. Both dinuclear Cu_2(μ-OAc)$_4$ and mononuclear $Cu(OAc)_2$ models were examined for each pathway. Figure 6 presents unrestricted MN15L (*46*) functional results. This method was chosen on the basis of its general accuracy for thermodynamics, barriers, and spin states for first-row transition metals. While there are no overall different mechanistic conclusions using alternative functionals [e.g., M06L (*47*)] and wave function methods [DLPNO-CCSD(T) (*48*–*49*)], the relative energies of structures do change (see the Supplementary Materials, Section S28 for comparison table S36).

Using the results of DFT calculations in combination with our experimental results (see above and the Supplementary Materials), we propose the reaction mechanism outlined by the calculated energy landscape for the para position of toluene shown in Fig. 6A (in black). In an initial step, Cu_2(μ-OAc)$_4$ (**1**) coordinates and activates a C—H bond of toluene (we modeled the para C—H bond) in a one-step metalation process to form (*p*-tolyl)Cu^{II}(HOAc)(μ-OAc)$_2$$Cu^{II}$(κ^2-OAc) (**2**) with a calculated Gibbs activation energy of 41.4 kcal mol^{-1} (at 170°C). This C—H activation step involves concerted formation of the Cu–*p*-tolyl bond with simultaneous proton transfer to the acetate ligand in a pathway (TS1). The structure TS1 shown in Fig. 6A is similar to many other transition states reported for arene C—H activation by metal acetate complexes and is often called concerted metalation deprotonation (*50*). The energies for TS1 at the ortho- and meta-positions of toluene are very similar (within 1.6 kcal mol^{-1} or closer) to the transition state energy for para C—H activation, which is consistent with the very small experimental selectivity (see Fig. 6B).

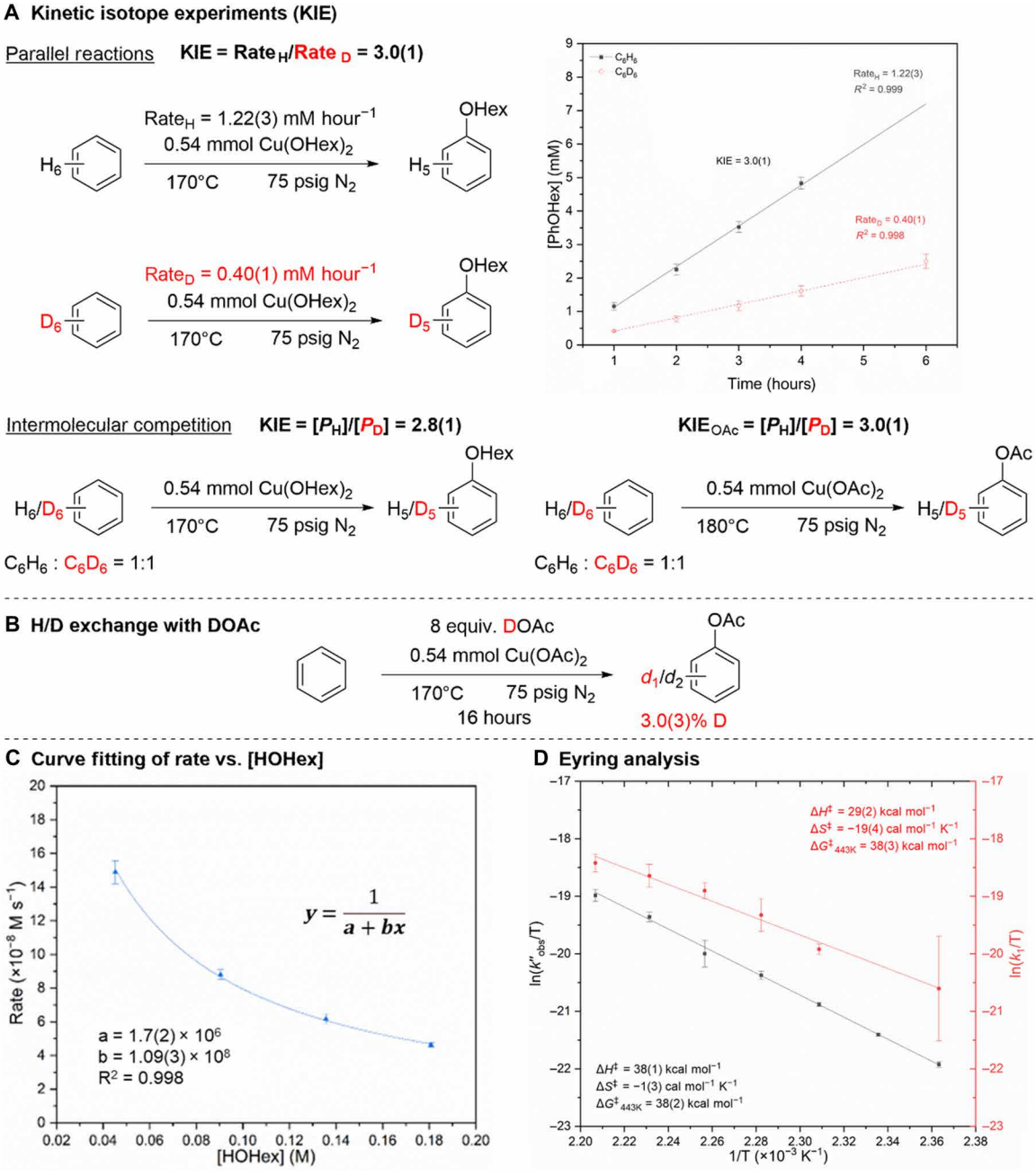

Fig. 5. Mechanistic studies. (**A**) Measurements of KIE using parallel reactions and intermolecular competition experiments. (**B**) H/D exchange experiment using acetic acid-d_1 (DOAc) as the deuterium source. (**C**) Curve fitting of observed reaction rates (rate) versus HOHex concentration plot for 2-ethylhexanoation of toluene using $Cu(OHex)_2$ with the addition of different amounts of HOHex at 170°C. (**D**) Eyring plot for toluene functionalization using $Cu(OHex)_2$ calculated with k_{obs} (in black) and k_1 (in red). Reaction rates were measured for production of tolyl OHex over the temperature range 150° to 180°C under the conditions with addition of variant amounts of HOHex. Rate equation: rate = k''_{obs}[toluene][Cu dimer]. The rate constant k_1 was calculated using curve fitting of observed reaction rates versus HOHex concentration.

Dissociation of HOAc precedes C—O reductive coupling between tolyl and acetate ligands (TS2), which occurs with a calculated Gibbs activation energy of 39.2 kcal mol^{-1} and forms (tolyl acetate)$Cu_2(\mu\text{-}OAc)_2$ (**5**). TS2 has a typical three-centered reductive coupling/elimination geometry where the Cu—OAc and Cu—Ar bonds are broken with simultaneous formation of the new C—O bond. Dissociation of the tolyl acetate from **5** gives the final organic product. Inspection of structure and bonding after HOAc dissociation and during the reductive elimination step suggests that this process occurs through a Cu(III)/Cu(I) intermediate rather than a Cu(II)/Cu(II) intermediate. This leads us to conclude that the second Cu atom is important in facilitating the C—O reductive coupling step by an intramolecular oxidation, a proposal that is consistent with calculated energetics using the monomeric $Cu(OAc)_2$ (**7**) species (see below and Fig. 6A in blue).

Figure 6A also shows a comparison of the dinuclear Cu pathway to arene activation by monomeric $Cu(OAc)_2$ (**7**), which is potentially

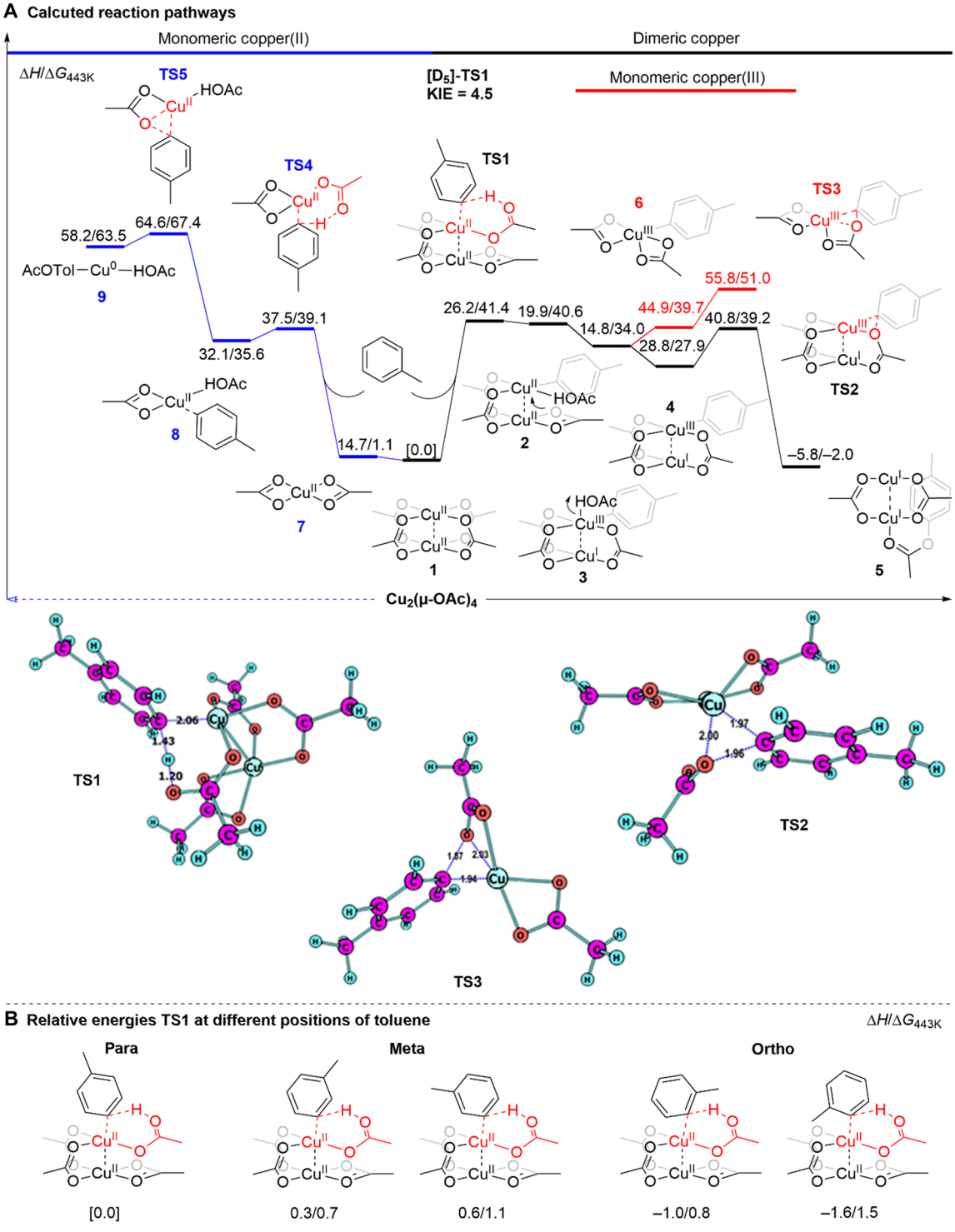

Fig. 6. Computational modeling of possible reaction pathways. (**A**) UMN15L/Def2-TZVPP//UMN15L/Def2-SVP calculated relative enthalpies and Gibbs energies (in kilocalories per mole) at 170°C of the calculated reaction pathways with $Cu_2(\mu\text{-}OAc)_4$ and $Cu(OAc)_2$ monomer. (**B**) Relative energies of ortho, para, and meta C—H activation transition states.

viable because the Gibbs energy for formation of the monomer only requires 1.1 kcal mol^{-1} relative to $Cu_2(\mu\text{-}OAc)_4$ (**1**). While the toluene C—H activation by monomeric $Cu(OAc)_2$ (**7**) has a Gibbs activation barrier close to the experimental value (39.1 kcal mol^{-1}), the calculated barrier (67.4 kcal mol^{-1}) for the C—O reductive coupling step is too high to be feasible. Therefore, a mononuclear Cu pathway would require conversion of the mononuclear Cu–*p*-tolyl (**8**) to a dinuclear structure for reductive elimination or aryl acetate product formation. However, the low concentration of the mononuclear Cu–*p*-tolyl structure (**8**) is because it is highly endothermic, which makes this

set of reaction steps unlikely. Another possible reaction pathway is C—H activation by $Cu(OAc)_2$ (**7**), followed by an intermolecular disproportionation to form a monomeric Cu(III) species **6** along with a Cu(I) compound, which avoids the high-energy aryl ester reductive elimination from the Cu(II) intermediate **8** (see above). The disproportionation pathway is similar to the previously proposed mechanism for directed Cu(II)-mediated C—H acetoxylation/hydroxylation (*13*, *16*). However, the calculated activation barrier for C—O reductive coupling from the monomeric Cu(III)-tolyl intermediate via TS3 (51.0 kcal mol^{-1}) indicates that this is an uncompetitive pathway. In addition, if the reaction undergoes the intermolecular disproportionation route, then the addition of 0.5 equivalents of ligand (e.g., bipyridine, tetramethyl ethylenediamine, etc.) might be expected to accelerate the reaction since the donor ligand could facilitate the oxidation of LCu(II)-tolyl to form the monomeric LCu(III)-tolyl intermediate; however, our data show that all ligands studied inhibit the $Cu_2(\mu\text{-}OAc)_4$-mediated organometallic arene functionalization.

The calculated activation enthalpy and Gibbs energies for the dinuclear Cu C—H activation step ($\Delta H^{\ddagger}$ = 26.2 kcal mol^{-1} and $\Delta G^{\ddagger}_{443K}$ = 41.4 kcal mol^{-1}) are consistent with the experimental values from the Eyring analysis using k_1 ($\Delta H^{\ddagger}$ = 29(2) kcal mol^{-1} and $\Delta G^{\ddagger}_{443K}$ = 38(3) kcal mol^{-1}). The calculated KIE for the C—H(D) activation transition state using deuterium at all five aromatic positions and corresponding zero-point energies is 4.5, which is slightly larger than but still consistent with the experimental KIE value of ~3.0, especially considering that zero-point energy is only one of several factors that control KIE values. In addition, the KIE study was measured on the basis of the overall rate of the reaction, instead of the individual rate constant k_1. The reductive coupling/elimination step has energies of $\Delta H^{\ddagger}$ = 40.8 kcal mol^{-1} and $\Delta G^{\ddagger}_{443K}$ = 39.2 kcal mol^{-1}. The nearly equal energies for C—H activation and reductive elimination suggest that both transition states may control the reaction rate and one transition state may dominate under specific conditions. This viewpoint provides an explanation for the observed primary KIE value, partially reversible C—H activation step, and possible overall rate-limiting reductive elimination with a small activation entropy. We propose that the C—H activation step is reversible; therefore, at low acid concentrations, the equilibrium of the C—H activation step may contribute to the isotope effect. There are several possible reasons for a very small activation entropy, and one possible origin is provided by the energy landscape. Figure 6A shows that the Gibbs energy for the reductive elimination transition state ($\Delta H^{\ddagger}$ = 40.8 kcal mol^{-1} and $\Delta G^{\ddagger}_{443K}$ = 39.2 kcal mol^{-1}) is very close to the barrier for C—H activation. This could be explained by a scenario where C—H activation, HOAc dissociation, and reductive elimination steps all contribute to control the reaction rate. This proposal is also consistent with the experimentally observed difference in $\Delta S^{\ddagger}$ when performing the Eyring analysis using k_{obs} and k_1, as well as the inverse first-order dependence of the reaction rate on acid concentration.

In addition to the mononuclear and dinuclear C—H activation reaction pathways outlined in Fig. 6, we also examined several other possible mechanisms for toluene C—H functionalization that are much less likely based on calculated energies. While details of these pathways are presented in the Supplementary Materials, it is useful to mention a few key alternative pathways. For example, outersphere single-electron transfer from toluene to Cu(II) requires >140 kcal mol^{-1} since Cu(II) is only a moderate oxidant, and the resulting charged species are not significantly stabilized in toluene solvent. In addition, we estimated innersphere one-electron transfer from the toluene π system to the Cu metal center using TD-DFT excitation energies calculated from the Cu-toluene π-coordination complex (Fig. 7). This excitation energy is 36.9 kcal mol^{-1}, and the orbitals responsible for this excitation are shown in Fig. 7 (π-orbital **70β** to the Cu-ligand antibonding orbital **71β**). While this excitation may be competitive with TS1, subsequent C—H activation from this excited state still require about 39.6 kcal mol^{-1} and therefore an overall barrier of >60 kcal mol^{-1} (for alternative pathways, see the Supplementary Materials for details), which suggests that electron transfer chemistry is not occurring. We also

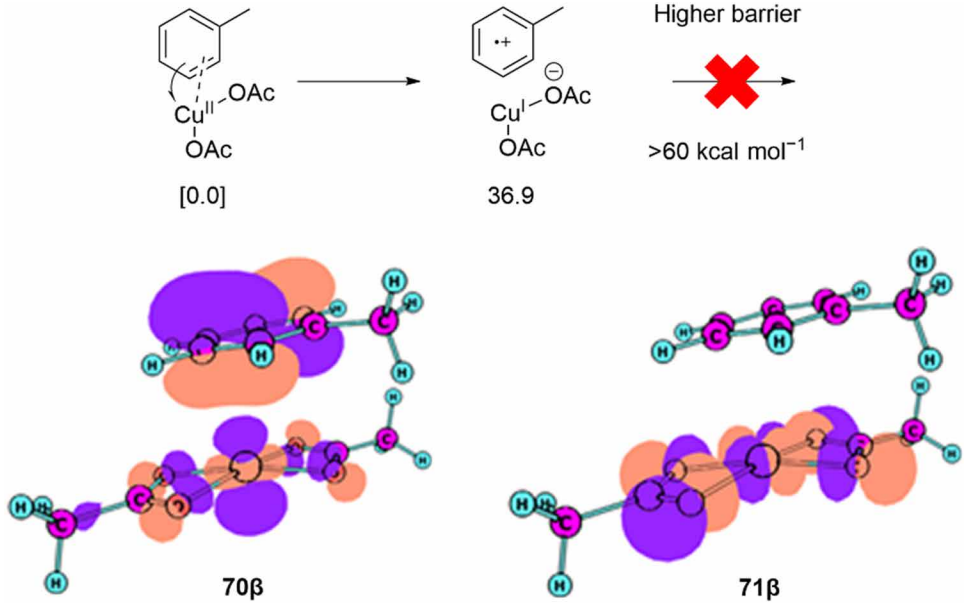

Fig. 7. Computational modeling of single-electron transfer pathways. UMN15L/Def2-TZVPP//MN15L/Def2-SVP Calculated energies for TD-DFT estimation for excitation between occupied orbital **70β** (toluene-centered) to unoccupied orbital **71β** (Cu-centered).

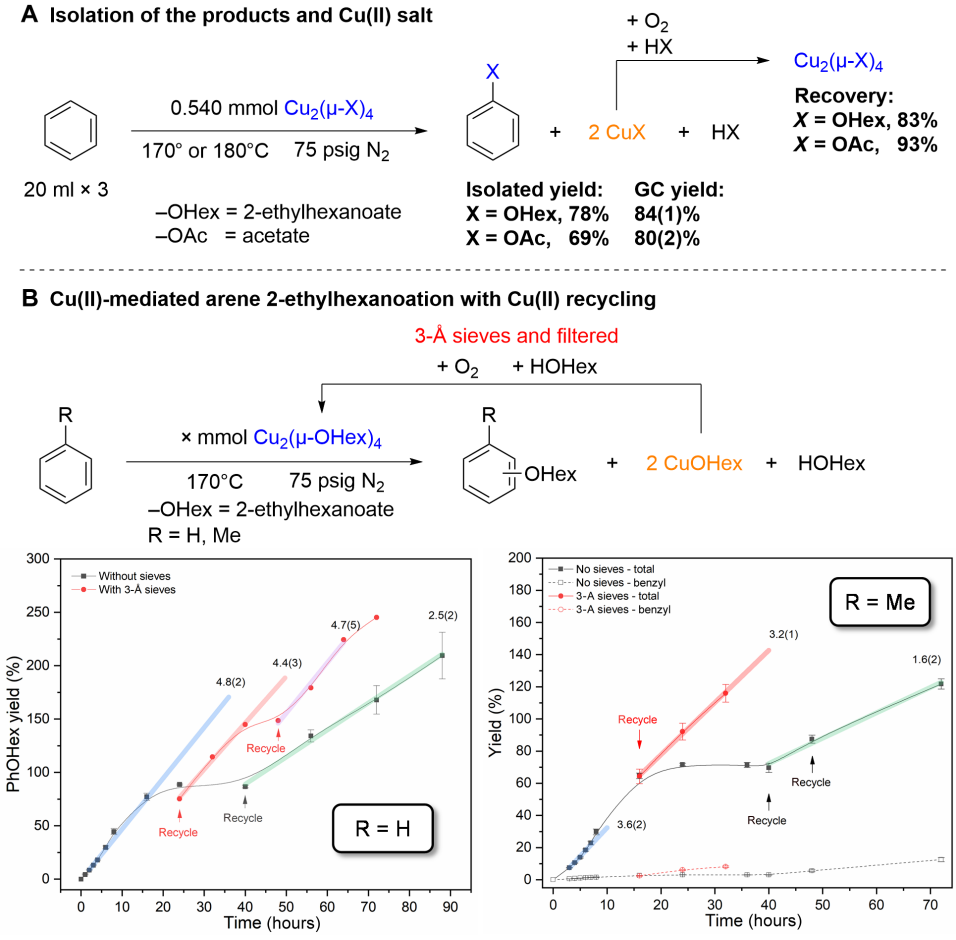

Fig. 8. Isolation of products and extension to Cu(II) recycling. (**A**) Isolation of the phenyl OHex/acetate product and recovery of the $Cu_2(\mu\text{-}X)_4$ used in the reaction. Reaction conditions: benzene (20 ml, 224.6 mmol), $Cu_2(\mu\text{-}X)_4$ [0.24 mol %, 0.540 mmol; $Cu_2(\mu\text{-}OAc)_4$, 196 mg; $Cu_2(\mu\text{-}OHex)_4$, 378 mg], under 75 psig of N_2 at 180°C for $Cu_2(\mu\text{-}OAc)_4$ and at 170°C for $Cu_2(\mu\text{-}OHex)_4$. (**B**) Cu(II)-mediated arene 2-ethylhexanoation with Cu(II) recycling. Reaction conditions: benzene (10 ml, 112.3 mmol), $Cu_2(\mu\text{-}OHex)_4$ (189 mg, 0.270 mmol), under 75 psig of N_2 at 170°C; toluene (10 ml, 94.1 mmol), $Cu_2(\mu\text{-}OHex)_4$ (158 mg, 0.226 mmol), under 75 psig of N_2 at 170°C. Yield of the phenyl carboxylate is relative to the limiting Cu reagent. SDs were calculated from at least three independent experiments.

considered reactions that proceed through the initial formation of radical species, such as ·OH or ·OAc. However, these pathways are unlikely based on calculated Gibbs energies, which require 52.8 and 60.5 kcal mol^{-1}, respectively, to form these radical species from the initial Cu complex.

Isolation of products and recycling of Cu(II)

The reaction using $Cu(OHex)_2$ was scaled to 1.1 g where 78% isolated yield of PhOHex and 83% recovery of the $Cu(OHex)_2$ were achieved (Fig. 8A). We demonstrated recycling of the recovered $Cu(OHex)_2$ using toluene as the substrate, and no difference in tolyl-to-benzyl selectivity was observed upon use of the recycled $Cu(OHex)_2$ (section S17.1). PhOAc can also be isolated with 69% yield along with 93% recovery of the used $Cu(OAc)_2$. With knowledge of the effect of molecular sieves, water, and O_2 (sections S10 to S12), we pursued a demonstration that the Cu(II) salt could be recovered and recycled after a completed reaction, similar in some ways to one version of the commercialized Wacker process (*32*–*35*). To do so, after each reaction, 0.5 equivalents of HOHex was added to the reaction solution and stirred under air until the solution turned dark blue, indicating that Cu(I) is oxidized to Cu(II). Then, 3-Å molecular sieves were added to remove the generated water that was formed from the regeneration of $Cu(OHex)_2$. After filtration to remove the sieves and trapped water, $Cu(OHex)_2$ was isolated and reused for the reaction under anaerobic conditions and demonstrated a similar rate as before either using benzene or toluene as the substrate (Fig. 8B), and 2.5 turnovers (TOs) (based on bis-Cu not monomeric Cu) of PhOHex can be achieved. The hydrolysis step of the phenyl carboxylate products was performed (section S21) using a previously reported procedure (*51*). In addition, phenol can be formed in >95% yield by reacting MeOH with phenyl carboxylate product, so that the formed methyl ester and remaining MeOH can be readily isolated from the reaction mixture by distillation. Overall, in the recycle experiments, 240% total yield from benzene to phenol was achieved [based on Cu(II)] with 0.6% total conversion of the initial benzene. By changing the molar ratio of benzene and Cu(II) salts along with using solvent, 2.4% conversion of benzene can be reached; however, there is likely a thermodynamic inhibition to achieving higher conversion (section S22).

DISCUSSION

We report a process using copper(II) carboxylate salts to oxidize benzene and toluene without installation of a directing group through a proposed organometallic Cu(II)-mediated C—H activation pathway. While Cu-mediated C—H activation to form intermediates with Cu—C bonds have been proposed previously (*13*, *15*), to our knowledge, evidence for nonradical Cu-mediated functionalization of hydrocarbons with strong C—H bonds is rare. Further, we have demonstrated that the copper(II) carboxylate salts used for the reaction can be isolated, recycled, and reused for the reaction with little change in reactivity, which is similar to one version of the commercial Wacker process for ethylene oxidation (*32*–*35*). Regeneration of the copper(II) carboxylate salt is achieved in solution using O_2 after each reaction, and with the removal of the generated water, the reaction maintains a similar rate using recycled Cu(II) (section S20). By adding a hydrolysis step of the phenyl carboxylate product, which is a known reaction (*51*), this process could provide a coproduct-free synthetic route for phenol production using cheap air-recyclable Cu(II) salts.

Our experimental and computational mechanistic studies demonstrate that the dimeric Cu(II) structure of $Cu_2(\mu\text{-}OAc)_4$ lowers the activation barrier for the product forming C—O reductive coupling step from the Cu(III)-Ar intermediate. This proposal shares some similarities to our previously published catalysis for styrene production using benzene and ethylene for which we propose the incorporation of Cu(II) in a Rh/Cu/Rh structure reduces the activation barrier for an O—H bond forming reductive coupling step (*52*). Thus, the incorporation of a Lewis acidic and oxidizing Cu(II) center (and possibly related metals) into a multimetallic species might represent a general strategy to facilitate catalytic hydrocarbon oxidation.

MATERIALS AND METHODS

General considerations

All reactions were performed under a dinitrogen atmosphere using Schlenk line techniques or inside a dinitrogen filled glovebox unless specified otherwise. GC-FID was performed using a Shimadzu GC-2014 system with a 30 m–by–0.25 mm DB-5ms capillary column with 0.25-μm film thickness. GC–mass spectrometry (MS) was performed using a Shimadzu GCMS-QP2010 Plus or a Shimadzu GCMS-QP2020 NX with a 30 m–by–0.25 mm Rxi-5ms capillary column with 0.25-μm film thickness using electron impact ionization method. Toluene was dried using sodium-benzophenone/ketyl stills under dinitrogen atmosphere and stored inside the glovebox. Methanol was dried using a calcium hydride still under dinitrogen atmosphere and stored inside a glovebox. Benzene, acetonitrile, and methylene chloride were dried using a solvent purification system with activated alumina. Toluene-d_8, acetonitrile-d_3, benzene-d_6, and methylene chloride-d_2 were dried and stored over activated 3-Å molecular sieves inside a glovebox. Except for the Cu(II) salts (see below), all other chemicals were purchased from commercial sources and used as received. Elemental analyses were performed by the University of Virginia Chemistry Department Elemental Analysis Facility.

General procedures for pretreatment of Cu(II) salts

The commercial Cu(II) salts was ground and heated in a Schlenk flask under ~10-mTorr vacuum in a 110°C oil bath for at least 1 day or 90°C for 3 days. During the drying process, the condensation of a colorless liquid was observed on the side of the round bottom flask, and a heat gun was used to completely transfer the liquid into the liquid dinitrogen trap on the Schlenk line. After drying, the needle valve was sealed, and the flask containing Cu(II) salts was directly transferred into the glovebox without opening to air.

Alternate method to purify $Cu(OHex)_2$

Commercial $Cu(OHex)_2$ (10 g) was dissolved in 60 ml of ethanol (EtOH) and stirred until a homogeneous solution was formed. Then, deionized water was added until no more precipitation. The mixture was filtered to collect the fine greenish-blue solid. After washing with water a few times, the solid was placed in a vacuum oven at 100°C until no mass change to yield the final product (9.3 g). This method particularly useful for removing high boiling point 2-ehtylhexanoic acid in the commercial $Cu(OHex)_2$. For more details, please see section S2.3.

Synthesis of $Cu(OHex)_2$

To a solution of NaOH (10 g, 250 mmol) in 300 ml of EtOH, OHex acid (42 ml, 263 mmol) was added and stirred for 2 hours at room temperature. Then, $Cu(NO_3)_2{\cdot}3H_2O$ (30.2 g, 125 mmol) was added to the solution. The color of the solution was blue and then changed to a greenish-blue color with solid precipitation. The mixture was then stirred at room temperature for at least 2 hours, and then deionized water was added to precipitate out the solid product as a greenish-blue fine solid. The solid was washed with deionized water to remove the water-soluble salts. Then, the solid product was placed in a vacuum oven-heated to 100° to 110°C under vacuum until no mass changes to yield the final $Cu(OHex)_2$ product (39.4 g, 90% isolated yield). The solid not only can be further dried using the same procedure described above but can also be used directly without further drying process.

Synthesis of $(MeO)_3P{=}O\ Cu(OAc)_2$

To a solution of $Cu(OAc)_2$ (100 mg, 0.551 mmol) in 5 ml of toluene, trimethyl phosphate (1 ml, 8.639 mmol) and 1 ml of HOAc were added. After heating at reflux for approximately 1 hour, the suspension was filtered hot to remove the undissolved $Cu(OAc)_2$ [most of the $Cu(OAc)_2$ was not dissolved], and crystals suitable for x-ray analysis were obtained by slow evaporation from light-blue filtrate (20 mg, 11% isolated yield). Combustion elemental analysis calculated (Anal. Calcd) for $C_{14}H_{30}O_{16}P_2Cu_2$: C, 26.13; H, 4.70. Found: trial#1, C, 25.84; H, 4.48; trial#2, C, 25.92; H, 4.49.

Synthesis of $(MeO)_3P{=}O\ Cu(OPiv)_2$

To a solution of $Cu(OPiv)_2$ (100 mg, 0.389 mmol) in 5 ml of toluene, trimethyl phosphate (45 μl, 0.389 mmol) was added. After heating at reflux for approximately 1 hour, the solution was filtered hot, and crystals suitable for x-ray analysis were obtained from slow evaporation from the blue filtrate (82 mg, 53% isolated yield). Anal. Calcd for $C_{26}H_{54}P_2O_{16}Cu_2$: C, 38.47; H, 6.71. Found: C, 38.53; H, 6.96.

General procedure for Cu(II)-mediated arene C—H acetoxylation

Under an atmosphere of dry dinitrogen inside a glovebox that the purity was maintained as $O_2 < 5$ parts per million (ppm) and $H_2O <$ 1 ppm, the copper(II) salt [CuX_2, X = OAc, 0.540 mmol (0.48 mol % to relative to benzene and 0.57 mol % relative to toluene); for soluble CuX_2, X = OPiv or OHex, 0.48 mol % relative to arene (0.540 mmol for reaction using benzene and 0.452 mmol for reaction using toluene)] was added into a dried Andrews Glass Lab-Crest Fisher-Porter tube with a stir bar, and then 10 ml of arene (benzene or toluene) was

measured by a syringe and added to the reaction tube. The Fisher-Porter tube was then sealed and pressurized with 75 psig of dinitrogen. Then, the mixture was stirred in an oil bath at reaction temperature (the oil bath temperature was confirmed by an external mercury thermometer), and the stir plate stirring speed was set to 550 rpm. The reaction time was recorded starting at the time the oil bath temperature reached the setting point, which typically required 5 to 10 min after placing the Fisher-Porter tube into the 1 liter of oil bath with 500 to 600 ml of silicone oil (usable range from −40° to 200°C). The reaction was monitored periodically by taking a 100-μl aliquot of the reaction solution, mixing with 100 μl of an HMB stock solution in arene (benzene or toluene) with known HMB concentration, and then quickly washing the mixture with saturated sodium hydroxide solution (~0.2 ml). The resulting organic layer was subjected to GC-FID and/or GC-MS for quantitative analysis, using relative peak areas versus HMB as the standard.

SUPPLEMENTARY MATERIALS

Supplementary material for this article is available at https://science.org/doi/10.1126/sciadv.add1594

REFERENCES AND NOTES

1. R. J. Schmidt, Industrial catalytic processes—Phenol production. *Appl. Catal. A Gen.* **280**, 89–103 (2005).
2. A. Mancuso, O. Sacco, D. Sannino, V. Venditto, V. Vaiano, One-step catalytic or photocatalytic oxidation of benzene to phenol: Possible alternative routes for phenol synthesis? *Catalysts* **10**, 1424 (2020).
3. K. H. Kuechler, F. M. Benitez, Dehydrogenation processes and phenol compositions. U.S. Patent 9,242,918 (2016).
4. H. Nair, C. L. Becker, R. A. Sothen, C. M. Smith, T.-J. Chen, Process for producing phenol. U.S. Patent 9,233,890 (2016).
5. W. D. McGhee, Selective introduction of active sites for hydroxylation of benzene. U.S. Patent 5,977,008 (1999).
6. H. Orita, T. Hayakawa, M. Shimizu, K. Takehira, Catalytic hydroxylation of benzene by the copper-ascorbic acid-O_2 system. *J. Mol. Catal.* **42**, 99–103 (1987).
7. T. Kitamura, H. Kanzaki, R. Hamada, S. Nishiyama, S. Tsuruya, Liquid-phase oxidation of benzene to phenol by copper catalysts in aqueous solvent with a high acetic acid concentration. *Can. J. Chem.* **82**, 1597–1605 (2004).
8. A. Häusser, M. Trautmann, E. Roduner, Spin trapping of hydroxyl radicals on Cu/HY zeolites suspended in aqueous solution. *Chem. Commun.* **47**, 6954–6956 (2011).
9. D. Wang, J. N. Jaworski, S. S. Stahl, Pd-catalyzed aerobic oxidation reactions: Industrial applications and new developments, in *Liquid Phase Aerobic Oxidation Catalysis: Industrial Applications and Academic Perspectives*, S. S. Stahl, P. L. Alsters, Eds. (Wiley-VCH, 2016), pp. 113–138.
10. S. R. Neufeldt, M. S. Sanford, Controlling site selectivity in palladium-catalyzed C–H bond functionalization. *Acc. Chem. Res.* **45**, 936–946 (2012).
11. T. Yoneyama, R. H. Crabtree, Pd(II) catalyzed acetoxylation of arenes with iodosyl acetate. *J. Mol. Catal. A Chem.* **108**, 35–40 (1996).
12. X. Chen, X.-S. Hao, C. E. Goodhue, J. Q. Yu, Cu(II)-catalyzed functionalizations of aryl C–H bonds using O_2 as an oxidant. *J. Am. Chem. Soc.* **128**, 6790–6791 (2006).
13. X. Li, Y.-H. Liu, W.-J. Gu, B. Li, F. J. Chen, B. F. Shi, Copper-mediated hydroxylation of arenes and heteroarenes directed by a removable bidentate auxiliary. *Org. Lett.* **16**, 3904–3907 (2014).
14. B. K. Singh, R. Jana, Ligand-enabled, copper-promoted regio- and chemoselective hydroxylation of arenes, aryl halides, and aryl methyl ethers. *J. Org. Chem.* **81**, 831–841 (2016).
15. S.-Z. Sun, M. Shang, H.-L. Wang, H. X. Lin, H. X. Dai, J. Q. Yu, Cu(II)-mediated C(sp2)–H hydroxylation. *J. Org. Chem.* **80**, 8843–8848 (2015).
16. A. M. Suess, M. Z. Ertem, C. J. Cramer, S. S. Stahl, Divergence between organometallic and single-electron-transfer mechanisms in copper(II)-mediated aerobic C–H oxidation. *J. Am. Chem. Soc.* **135**, 9797–9804 (2013).
17. J. Gallardo-Donaire, R. Martin, Cu-catalyzed mild C(sp2)–H functionalization assisted by carboxylic acids en route to hydroxylated arenes. *J. Am. Chem. Soc.* **135**, 9350–9353 (2013).
18. W. Wang, F. Luo, S. Zhang, J. Cheng, Copper(II)-catalyzed ortho-acyloxylation of the 2-arylpyridines sp^2 C–H bonds with anhydrides, using O_2 as terminal oxidant. *J. Org. Chem.* **75**, 2415–2418 (2010).
19. M. Shang, Q. Shao, S.-Z. Sun, Y. Q. Chen, H. Xu, H. X. Dai, J. Q. Yu, Identification of monodentate oxazoline as a ligand for copper-promoted ortho-C–H hydroxylation and amination. *Chem. Sci.* **8**, 1469–1473 (2017).
20. X. Wu, Y. Zhao, H. Ge, Pyridine-enabled copper-promoted cross dehydrogenative coupling of C(sp2)–H and unactivated C(sp3)–H bonds. *Chem. Sci.* **6**, 5978–5983 (2015).
21. X. Zeng, W. Yan, M. Paeth, S. B. Zacate, P. H. Hong, Y. Wang, D. Yang, K. Yang, T. Yan, C. Song, Z. Cao, M. J. Cheng, W. Liu, Copper-catalyzed, chloroamide-directed benzylic C–H difluoromethylation. *J. Am. Chem. Soc.* **141**, 19941–19949 (2019).
22. D. K. Pandey, A. B. Shabade, B. Punji, Copper-catalyzed direct arylation of indoles and related (hetero)arenes: A ligandless and solvent-free approach. *Adv. Synth. Catal.* **362**, 2534–2540 (2020).
23. R. Odani, K. Hirano, T. Satoh, M. Miura, Copper-mediated formally dehydrative biaryl coupling of azine N-oxides and oxazoles. *J. Org. Chem.* **80**, 2384–2391 (2015).
24. M. Nishino, K. Hirano, T. Satoh, M. Miura, Copper-mediated and copper-catalyzed cross-coupling of indoles and 1,3-azoles: Double C–H activation. *Angew. Chem. Int. Ed.* **51**, 6993–6997 (2012).
25. K. Takamatsu, Y. Hayashi, S. Kawauchi, K. Hirano, M. Miura, Copper-catalyzed regioselective C–H amination of phenol derivatives with assistance of phenanthroline-based bidentate auxiliary. *ACS Catal.* **9**, 5336–5344 (2019).
26. M. Shang, S.-Z. Sun, H.-X. Dai, J. Q. Yu, $Cu(OAc)_2$-catalyzed coupling of aromatic C–H bonds with arylboron reagents. *Org. Lett.* **16**, 5666–5669 (2014).
27. C. Yamamoto, K. Takamatsu, K. Hirano, M. Miura, Copper-catalyzed intramolecular benzylic C–H amination for the synthesis of isoindolinones. *J. Org. Chem.* **81**, 7675–7684 (2016).
28. M. Shang, S.-Z. Sun, H.-L. Wang, B. N. Laforteza, H. X. Dai, J. Q. Yu, Exceedingly fast copper(II)-promotedortho C–H trifluoromethylation of arenes using TMSCF3. *Angew. Chem. Int. Ed.* **53**, 10439–10442 (2014).
29. X. Wu, J. Miao, Y. Li, G. Li, H. Ge, Copper-promoted site-selective carbonylation of sp^3 and sp^2 C–H bonds with nitromethane. *Chem. Sci.* **7**, 5260–5264 (2016).
30. R. Wang, Y. Li, R.-X. Jin, X. S. Wang, Copper-catalyzed oxidative $C(sp^3)$–H/$C(sp^2)$–H cross-coupling en route to carbocyclic rings. *Chem. Sci.* **8**, 3838–3842 (2017).
31. J. Wang, R. Sang, X. Chong, Y. Zhao, W. Fan, Z. Li, J. Zhao, Copper-catalyzed radical cascade oxyalkylation of olefinic amides with simple alkanes: Highly efficient access to benzoxazines. *Chem. Commun.* **53**, 7961–7964 (2017).
32. J. A. Keith, P. M. Henry, The mechanism of the wacker reaction: A tale of two hydroxypalladations. *Angew. Chem. Int. Ed.* **48**, 9038–9049 (2009).
33. J. Smidt, W. Hafner, R. Jira, J. Sedlmeier, R. Sieber, R. Rüttinger, H. Kojer, Katalytische Umsetzungen von Olefinen an Platinmetall-Verbindungen Das Consortium-Verfahren zur Herstellung von Acetaldehyd. *Angew. Chem.* **71**, 176–182 (1959).
34. G. F. M. Eckert, R. Jira, H. M. Bolt, K. Golka, in *Ullmann's Encyclopedia of Industrial Chemistry* (Wiley-VCH Verlag, 2000), pp 1–17.
35. Hoechst reveals wacker process details. *Chem. Eng. News* **39**, 52–55 (1961).
36. J. Chen, R. J. Nielsen, W. A. Goddard III, B. A. McKeown, D. A. Dickie, T. B. Gunnoe, Catalytic synthesis of superlinear alkenyl arenes using a Rh(I) catalyst supported by a "Capping Arene" ligand: Access to aerobic catalysis. *J. Am. Chem. Soc.* **140**, 17007–17018 (2018).
37. F. Kong, S. Gu, C. Liu, D. A. Dickie, S. Zhang, T. B. Gunnoe, Effects of additives on catalytic arene C–H activation: Study of Rh catalysts supported by bis-phosphine pincer ligands. *Organometallics* **39**, 3918–3935 (2020).
38. D. Munz, M. Webster-Gardiner, R. Fu, T. Strassner, W. A. Goddard III, T. B. Gunnoe, Proton or metal? The H/D exchange of arenes in acidic solvents. *ACS Catal.* **5**, 769–775 (2015).
39. C. E. Elwell, N. L. Gagnon, B. D. Neisen, D. Dhar, A. D. Spaeth, G. M. Yee, W. B. Tolman, Copper–oxygen complexes revisited: Structures, spectroscopy, and reactivity. *Chem. Rev.* **117**, 2059–2107 (2017).
40. L. M. Mirica, X. Ottenwaelder, T. D. P. Stack, Structure and spectroscopy of copper–dioxygen complexes. *Chem. Rev.* **104**, 1013–1046 (2004).
41. E. A. Lewis, W. B. Tolman, Reactivity of dioxygen–copper systems. *Chem. Rev.* **104**, 1047–1076 (2004).
42. A. Conde, L. Vilella, D. Balcells, M. M. Díaz-Requejo, A. Lledós, P. J. Pérez, Introducing copper as catalyst for oxidative alkane dehydrogenation. *J. Am. Chem. Soc.* **135**, 3887–3896 (2013).
43. P. Sharrock, M. Melník, Copper(II) acetates: From dimer to monomer. *Can. J. Chem.* **63**, 52–56 (1985).
44. E. M. Simmons, J. F. Hartwig, On the interpretation of deuterium kinetic isotope effects in C–H bond functionalizations by transition-metal complexes. *Angew. Chem. Int. Ed.* **51**, 3066–3072 (2012).
45. W. D. Jones, Isotope effects in C–H bond activation reactions by transition metals. *Acc. Chem. Res.* **36**, 140–146 (2003).
46. H. S. Yu, X. He, D. G. Truhlar, MN15-L: A new local exchange-correlation functional for Kohn–Sham density functional theory with broad accuracy for atoms, molecules, and solids. *J. Chem. Theory Comput.* **12**, 1280–1293 (2016).

47. Y. Zhao, D. G. Truhlar, A new local density functional for main-group thermochemistry, transition metal bonding, thermochemical kinetics, and noncovalent interactions. *J. Chem. Phys.* **125**, 194101 (2006).
48. C. Riplinger, B. Sandhoefer, A. Hansen, F. Neese, Natural triple excitations in local coupled cluster calculations with pair natural orbitals. *J. Chem. Phys.* **139**, 134101 (2013).
49. C. Riplinger, F. Neese, An efficient and near linear scaling pair natural orbital based local coupled cluster method. *J. Chem. Phys.* **138**, 034106 (2013).
50. D. L. Davies, S. A. Macgregor, C. L. McMullin, Computational studies of carboxylate-assisted C–H activation and functionalization at group 8–10 transition metal centers. *Chem. Rev.* **117**, 8649–8709 (2017).
51. W. Medina-Ramos, M. A. Mojica, E. D. Cope, R. J. Hart, P. Pollet, C. A. Eckert, C. L. Liotta, Water at elevated temperatures (WET): Reactant, catalyst, and solvent in the selective hydrolysis of protecting groups. *Green Chem.* **16**, 2147–2155 (2014).
52. C. B. Musgrave, W. Zhu, N. Coutard, J. F. Ellena, D. A. Dickie, T. B. Gunnoe, W. A. Goddard III, Mechanistic studies of styrene production from benzene and ethylene using $[(\eta^2\text{-}C_2H_4)_2Rh(\mu\text{-}OAc)]_2$ as catalyst precursor: Identification of a Bis-Rh^{I} Mono-Cu^{II} complex as the catalyst. *ACS Catal.* **11**, 5688–5702 (2021).
53. G. R. Fulmer, A. J. M. Miller, N. H. Sherden, H. E. Gottlieb, A. Nudelman, B. M. Stoltz, J. E. Bercaw, K. I. Goldberg, NMR chemical shifts of trace impurities: Common laboratory solvents, organics, and gases in deuterated solvents relevant to the organometallic chemist. *Organometallics* **29**, 2176–2179 (2010).
54. L.-H. Xie, M. P. Suh, Flexible metal–organic framework with hydrophobic pores. *Chem. A Eur. J.* **17**, 13653–13656 (2011).
55. D. S. Schrage, D. C. Malarik, A novel quartz dendritic growth chamber for low temperature microgravity experimentation. *Rev. Sci. Instrum.* **70**, 4624–4633 (1999).
56. A. Bruylants, M. Tits, C. Dieu, R. Gauthier, Directed chlorination. II. Aliphatic acids and nitriles, alkyl acetates. *Bull. Soc. Chim. Belg.* **61**, 366–392 (1952).
57. J. G. Traynham, M. A. Battiste, Solvolyses of some sterically hindered aliphatic esters1. *J. Org. Chem.* **22**, 1551–1554 (1957).
58. P. A. Levene, F. A. Taylor, On oxidation of tertiary hydrocarbons. *J. Biol. Chem.* **54**, 351–362 (1922).
59. A. L. J. Beckwith, Reactions of alkoxy radicals. I. The reactions of di-tert.-butyl peroxide with n-butyric acid and ethyl n-butyrate. *Aust. J. Chem.* **13**, 244–255 (1960).
60. S. Bette, A. Costes, R. K. Kremer, G. Eggert, C. C. Tang, R. E. Dinnebier, On verdigris, part III: Crystal structure, magnetic and spectral properties of anhydrous copper(II) acetate, a paddle wheel chain. *Z. Anorg. Allg. Chem.* **645**, 988–997 (2019).
61. E. O. Pentsak, D. B. Eremin, E. G. Gordeev, V. P. Ananikov, Phantom reactivity in organic and catalytic reactions as a consequence of microscale destruction and contamination-trapping effects of magnetic stir bars. *ACS Catal.* **9**, 3070–3081 (2019).
62. T. Jintoku, K. Takaki, Y. Fujiwara, Y. Fuchita, K. Hiraki, Palladium catalyzed direct oxidation of benzene with molecular oxygen to phenol. *Bull. Chem. Soc. Jpn.* **63**, 438–441 (1990).
63. M. Okamoto, T. Yamaji, A selective synthesis of biphenyl by the $Pd(Oac)_2/MoO_2(acac)_2/O_2$/AcOH catalyst system. *Chem. Lett.* **30**, 212–213 (2001).
64. A. R. Dick, K. L. Hull, M. S. Sanford, A highly selective catalytic method for the oxidative functionalization of C–H bonds. *J. Am. Chem. Soc.* **126**, 2300–2301 (2004).
65. L. V. Desai, K. J. Stowers, M. S. Sanford, Insights into directing group ability in palladium-catalyzed C–H bond functionalization. *J. Am. Chem. Soc.* **130**, 13285–13293 (2008).
66. N. R. Deprez, M. S. Sanford, Synthetic and mechanistic studies of Pd-catalyzed C–H arylation with diaryliodonium salts: Evidence for a bimetallic high oxidation state Pd intermediate. *J. Am. Chem. Soc.* **131**, 11234–11241 (2009).
67. D. C. Powers, M. A. L. Geibel, J. E. M. N. Klein, T. Ritter, Bimetallic palladium catalysis: Direct observation of Pd(III)–Pd(III) intermediates. *J. Am. Chem. Soc.* **131**, 17050–17051 (2009).
68. J. M. Racowski, A. R. Dick, M. S. Sanford, Detailed Study of C–O and C–C bond-forming reductive elimination from stable $C_2N_2O_2$–ligated palladium(IV) complexes. *J. Am. Chem. Soc.* **131**, 10974–10983 (2009).
69. K. J. Stowers, M. S. Sanford, Mechanistic comparison between Pd-catalyzed ligand-directed C–H chlorination and C–H acetoxylation. *Org. Lett.* **11**, 4584–4587 (2009).
70. D. C. Powers, D. Y. Xiao, M. A. L. Geibel, T. Ritter, On the mechanism of palladium-catalyzed aromatic C–H oxidation. *J. Am. Chem. Soc.* **132**, 14530–14536 (2010).
71. M. H. Emmert, A. K. Cook, Y. J. Xie, M. S. Sanford, Remarkably high reactivity of $Pd(OAc)_2$/pyridine catalysts: Nondirected C–H oxygenation of arenes. *Angew. Chem. Int. Ed.* **50**, 9409–9412 (2011).
72. J. Pei, S. Qin, G.-y. Li, C. W. Hu, Water-promoted one-step anodic acetoxylation of benzene to phenyl acetate with high selectivity. *Chin. J. Chem. Phys.* **24**, 244–248 (2011).
73. N. Wang, T. M. McCormick, S.-B. Ko, S. Wang, Pt^{II} and Pd^{II} complexes with a *trans*-chelating bis(pyridyl) ligand. *Eur. J. Inorg. Chem.* **2012**, 4463–4469 (2012).
74. A. K. Cook, M. H. Emmert, M. S. Sanford, Steric control of site selectivity in the Pd-catalyzed C–H acetoxylation of simple arenes. *Org. Lett.* **15**, 5428–5431 (2013).
75. J. B. Gary, A. K. Cook, M. S. Sanford, Palladium catalysts containing pyridinium-substituted pyridine ligands for the C–H oxygenation of benzene with $K_2S_2O_8$. *ACS Catal.* **3**, 700–703 (2013).
76. A. K. Cook, M. S. Sanford, Mechanism of the palladium-catalyzed arene C–H acetoxylation: A comparison of catalysts and ligand effects. *J. Am. Chem. Soc.* **137**, 3109–3118 (2015).
77. S. P. Desai, M. Mondal, J. Choudhury, Chelating bis-N-heterocyclic carbene–palladium(II) complexes for oxidative arene C–H functionalization. *Organometallics* **34**, 2731–2736 (2015).
78. S. L. Zultanski, S. S. Stahl, Palladium-catalyzed aerobic acetoxylation of benzene using NO_x-based redox mediators. *J. Organomet. Chem.* **793**, 263–268 (2015).
79. H. M. D. Bandara, D. Jin, M. A. Mantell, K. D. Field, A. Wang, R. P. Narayanan, N. A. Deskins, M. H. Emmert, Non-directed aromatic C–H amination: Catalytic and mechanistic studies enabled by Pd catalyst and reagent design. *Cat. Sci. Technol.* **6**, 5304–5310 (2016).
80. L. Li, Y. Wang, T. Yang, Q. Zhang, D. Li, Palladium-catalyzed non-directed CH benzoxylation of simple arenes with iodobenzene dibenzoates. *Tetrahedron Lett.* **57**, 5859–5863 (2016).
81. C. Valderas, K. Naksomboon, M. Á. Fernández-Ibáñez, Ligand-promoted palladium-catalyzed C–H acetoxylation of simple arenes. *ChemCatChem* **8**, 3213–3217 (2016).
82. M. H. Majeed, P. Shayesteh, L. R. Wallenberg, A. R. Persson, N. Johansson, L. Ye, J. Schnadt, O. F. Wendt, Polymer-supported palladium(II) carbene complexes: Catalytic activity, recyclability, and selectivity in C–H acetoxylation of arenes. *Chem. A Eur. J.* **23**, 8457–8465 (2017).
83. K. Naksomboon, C. Valderas, M. Gómez-Martínez, Y. Álvarez-Casao, M. Á. Fernández-Ibáñez, S,O-ligand-promoted palladium-catalyzed C–H functionalization reactions of nondirected arenes. *ACS Catal.* **7**, 6342–6346 (2017).
84. A. Shrestha, M. Lee, A. L. Dunn, M. S. Sanford, Palladium-catalyzed C–H bond acetoxylation via electrochemical oxidation. *Org. Lett.* **20**, 204–207 (2018).
85. D. Lapointe, K. Fagnou, Overview of the mechanistic work on the concerted metallation–deprotonation pathway. *Chem. Lett.* **39**, 1118–1126 (2010).
86. M. J. Frisch, G. W. Trucks, H. B. Schlegel, G. E. Scuseria, M. A. Robb, J. R. Cheeseman, G. Scalmani, V. Barone, G. A. Petersson, H. Nakatsuji, X. Li, M. Caricato, A. V. Marenich, J. Bloino, B. G. Janesko, R. Gomperts, B. Mennucci, H. P. Hratchian, J. V. Ortiz, A. F. Izmaylov, J. L. Sonnenberg, D. Williams-Young, F. Ding, F. Lipparini, F. Egidi, J. Goings, B. Peng, A. Petrone, T. Henderson, D. Ranasinghe, V. G. Zakrzewski, J. Gao, N. Rega, G. Zheng, W. Liang, M. Hada, M. Ehara, K. Toyota, R. Fukuda, J. Hasegawa, M. Ishida, T. Nakajima, Y. Honda, O. Kitao, H. Nakai, T. Vreven, K. Throssell, J. A. Montgomery, Jr., J. E. Peralta, F. Ogliaro, M. J. Bearpark, J. J. Heyd, E. N. Brothers, K. N. Kudin, V. N. Staroverov, T. A. Keith, R. Kobayashi, J. Normand, K. Raghavachari, A. P. Rendell, J. C. Burant, S. S. Iyengar, J. Tomasi, M. Cossi, J. M. Millam, M. Klene, C. Adamo, R. Cammi, J. W. Ochterski, R. L. Martin, K. Morokuma, O. Farkas, J. B. Foresman, D. J. Fox, *Gaussian 16 Rev. C.01* (Gaussian Inc., 2016).
87. F. Weigend, R. Ahlrichs, Balanced basis sets of split valence, triple zeta valence and quadruple zeta valence quality for H to Rn: Design and assessment of accuracy. *PCCP* **7**, 3297–3305 (2005).
88. F. Weigend, Accurate Coulomb-fitting basis sets for H to Rn. *Phys. Chem. Chem. Phys.* **8**, 1057–1065 (2006).
89. J. Zheng, X. Xu, D. G. Truhlar, Minimally augmented Karlsruhe basis sets. *Theor. Chem. Acc.* **128**, 295–305 (2011).
90. F. Neese, Software update: The ORCA program system, version 4.0. *WIREs Comput. Mol. Sci.* **8**, e1327 (2018).
91. R. L. Carlin, in *Magnetochemistry* (Springer Berlin Heidelberg, 1986), pp. 77–82.
92. J. Pipek, P. G. Mezey, A fast intrinsic localization procedure applicable for ab initio and semiempirical linear combination of atomic orbital wave functions. *J. Chem. Phys.* **90**, 4916–4926 (1989).
93. T. Lu, F. Chen, Multiwfn: A multifunctional wavefunction analyzer. *J. Comput. Chem.* **33**, 580–592 (2012).
94. Y. Kanazawa, T. Mitsudome, H. Takaya, M. Hirano, Pd/Cu-catalyzed dehydrogenative coupling of dimethyl phthalate: Synchrotron radiation sheds Light on the Cu cycle mechanism. *ACS Catal.* **10**, 5909–5919 (2020).
95. V. R. Yatham, W. Harnying, D. Kootz, J. M. Neudörfl, N. E. Schlörer, A. Berkessel, 1,4-bis-dipp/mes-1,2,4-triazolylidenes: Carbene catalysts that efficiently overcome steric hindrance in the redox esterification of α- and β-substituted α,β-enals. *J. Am. Chem. Soc.* **138**, 2670–2677 (2016).
96. W. Harnying, P. Sudkaow, A. Biswas, A. Berkessel, N-heterocyclic carbene/carboxylic acid co-catalysis enables oxidative esterification of demanding aldehydes/enals, at low catalyst loading. *Angew. Chem. Int. Ed.* **60**, 19631–19636 (2021).
97. N. Moszner, J. Angermann, U. Fischer, A. Gianasmidis, M. Tabatabai, H. Ritter, A. Utterodt, Methacrylated Calix[6]arenes as low shrinking additives for dental restorative composites. *Macromol. Mater. Eng.* **296**, 937–943 (2011).
98. C. B. Rao, B. Chinnababu, Y. Venkateswarlu, An efficient protocol for alcohol protection under solvent- and catalyst-free conditions. *J. Org. Chem.* **74**, 8856–8858 (2009).
99. K. W. Quasdorf, X. Tian, N. K. Garg, Cross-coupling reactions of aryl pivalates with boronic acids. *J. Am. Chem. Soc.* **130**, 14422–14423 (2008).
100. T. Liu, X. Shao, Y. Wu, Q. Shen, Highly selective trifluoromethylation of 1,3-disubstituted arenes through iridium-catalyzed arene borylation. *Angew. Chem. Int. Ed.* **51**, 540–543 (2012).

101. W. M. Czaplik, S. Grupe, M. Mayer, A. J. Wangelin, Practical iron-catalyzed dehalogenation of aryl halides. *Chem. Commun.* **46**, 6350–6352 (2010).
102. Bruker, *Saint; SADABS; APEX3* (Bruker AXS Inc., 2012).
103. G. M. Sheldrick, SHELXT - Integrated space-group and crystal-structure determination. *Acta Crystallogr. A Found. Adv.* **A71**, 3–8 (2015).
104. O. V. Dolomanov, L. J. Bourhis, R. J. Gildea, J. A. K. Howard, H. Puschmann, OLEX2: A complete structure solution, refinement and analysis program. *J. Appl. Cryst.* **42**, 339–341 (2009).
105. G. Sheldrick, *CELL_NOW, Version 2008/4* (Georg-August-Universität Göttingen, 2008).
106. A. Singh, A. Tiwari, S. M. Mahajani, R. D. Gudi, Recovery of acetic acid from aqueous solutions by reactive distillation. *Ind. Eng. Chem. Res.* **45**, 2017–2025 (2006).

Acknowledgments: We thank X. Jia for assistance with GC-MS analysis for the KIE studies and K. Zhang for assistance with statistical analysis. We thank S.-W. Yu for assistance with inductively coupled plasma optical emission spectrometry analysis. We thank Brigham Young University and the Office of Research Computing, especially the Fulton Supercomputing Laboratory. **Funding:** Experimental works was supported by the U.S. National Science Foundation under award CHE-2102433. Computational work was supported by the U.S. National Science Foundation Chemical Catalysis (CAT) Program under award CHE-2153215. **Author contributions:** Conceptualization: T.B.G. conceived the project. Methodology: T.B.G. and F.K. designed the experiments. D.H.E. and S.C. designed the computational simulations. J.C. performed preliminary experimental designs. Investigation: F.K. performed the experiments and analyzed experimental data with the help from C.L. and D.A.D. J.C. performed preliminary experimental studies. D.H.E. and S.C. provided computational simulation. W.Z. performed an experiment to isolate a single-crystal of $Cu(OPiv)_2$. Funding acquisition: T.B.G. and D.H.E. Supervision: T.B.G., D.H.E., S.Z., and W.L.S. Writing (original draft): F.K. and S.C. Writing (review and editing): T.B.G., D.H.E., F.K., S.C., D.A.D., J.C., C.L., and W.Z. **Competing interests:** T.B.G., J.C., F.K., and W.L.S. are inventors on a provisional patent application submitted by the University of Virginia that covers the method for producing an aryl ester by reacting arene with Cu(II) carboxylate, including air/dioxygen recycling steps, as well as Cu(II)-mediated conversion of arenes and alkenes to esters, alcohols, and aldehyde products. The authors declare that they have no other competing interests. **Data and materials availability:** All data are available in the main text or the Supplementary Materials. CCDC 2111796-2111797 contains the supplementary crystallographic data for this paper. These data can be obtained free of charge from the Cambridge Crystallographic Data Centre via www.ccdc.cam.ac.uk/structures.

Submitted 24 May 2022
Accepted 11 July 2022
Published 24 August 2022
10.1126/sciadv.add1594